Since January 2020 Elsevier has created a COVID-19 resource centre with free information in English and Mandarin on the novel coronavirus COVID-19. The COVID-19 resource centre is hosted on Elsevier Connect, the company's public news and information website.

Journal of Aerosol Science 41 (2010) 944–952

Contents lists available at ScienceDirect

Journal of Aerosol Science

journal homepage: www.elsevier.com/locate/jaerosci

Method for contamination of filtering facepiece respirators by deposition of MS2 viral aerosols

Myung-Heui Woo [a], Yu-Mei Hsu [b], Chang-Yu Wu [a,*], Brian Heimbuch [c], Joseph Wander [d]

[a] Department of Environmental Engineering Sciences, University of Florida, P.O. Box 116450, Gainesville, FL 32611-6450, USA
[b] Wood Buffalo Environmental Association, Alberta, Canada
[c] Applied Research Associates, Tyndall Air Force Base, FL, USA
[d] Air Force Research Laboratory, Tyndall Air Force Base, FL, USA

ARTICLE INFO

Article history:
Received 11 December 2009
Received in revised form
28 June 2010
Accepted 5 July 2010

Keywords:
Loading chamber
Coughing
Loading density
Uniformity
Droplet

ABSTRACT

A droplet/aerosol loading chamber was designed to deliver uniform droplets/aerosols onto substrates. An ultrasonic nebulizer was used to produce virus-containing droplets from artificial saliva to emulate those from coughing and sneezing. The operating conditions were determined by adjusting various parameters to achieve loading density and uniformity requirements. The count median diameter and mass median diameter were 0.5–2 and 3–4 μm, respectively, around the loading location when 35% relative humidity was applied. The average loading density was $\sim 2 \times 10^3$ plaque-forming units/cm^2 for 5-min loading time with a virus titer of 10^7 plaque-forming units/mL. Six different filtering facepiece respirators from commercial sources were loaded to evaluate uniform distribution. For each of the six FFRs, the virus loading uniformity within a sample and across numerous samples was 19.21% and 12.20%, respectively. This system supports a standard method for loading viable bioaerosols onto specimen surfaces when different decontamination techniques are to be compared.

1. Introduction

The public's concern about bioterrorism (e.g., the 2001 anthrax attack) and spread of airborne pathogens (e.g., Severe Acute Respiratory Syndrome (SARS) and avian flu (H5N1)) through the aerosol route has increased greatly in recent years (Tellier, 2006). For example, in 2002 and 2003, SARS caused over 8000 illnesses and 700 deaths, and there is still no adequate treatment (Yang, Lee, Chen, Wu, & Yu, 2007). The recent swine flu outbreak due to a new strain of H1N1 influenza A has caused illness in over 214 countries and resulted in 18311 deaths worldwide as of July 2010 (WHO, 2010). On June 11, 2009, the World Health Organization (WHO) raised the pandemic alert level to Phase 6, indicating the onset of a global pandemic (CDC, 2009).

One effective method for protection against airborne pathogens during pandemic spread through droplet and aerosol transmission is to wear a filtering facepiece respirator (FFR) certified by National Institute for Occupational Safety and Health (NIOSH). This approach considerably decreases the incidence and severity of infection. The Center for Disease Control and Prevention (CDC) has issued guidelines about the use of face masks and respirators to protect against H1N1 transmission in healthcare facilities (CDC, 2009). However, using medical masks and N95 FFRs as countermeasures for bioaerosols has not been demonstrated to provide a complete response: (1) although using surgical masks and N95 FFRs

* Corresponding author. Tel.: +1 352 392 0845; fax: +1 352 392 3076.
E-mail address: cywu@ufl.edu (C.-Y. Wu).

0021-8502/$ - see front matter © 2010 Elsevier Ltd. All rights reserved.
doi:10.1016/j.jaerosci.2010.07.003

for tuberculosis has been shown to meet CDC guidelines, the same is not true for viral agents such as the swine flu virus. (2) There is no experimental basis upon which the FFR's life span in an H1N1 scenario can be estimated. (3) The stockpile of FFRs will be exhausted in the event of a severe pandemic. CDC estimates that more than 90 million FFRs will be required for healthcare workers in the US if a pandemic influenza event persists for 42 days (CDRF, 2006).

One possible approach to resolve insufficient supplies of FFRs is to decontaminate the FFRs by applying disinfecting agents/processes, such as microwave irradiation, ultraviolet germicidal irradiation (UVGI), bleach solution, peroxides, etc., and then reusing the decontaminated respirator. To qualify a method to decontaminate an FFR for reuse, one must provide a statistically robust demonstration that the technologies applied do not alter the mechanical properties of the FFR, do not leave any toxic byproduct on the FFR, and achieve at least four-log virucidal efficacy on the materials of construction of the FFR. However, no protocol has been reported for such decontamination testing, a consequence of two main limitations. First, no standard test method has been reported for simulating bioaerosol contamination of the FFRs. Second, the unique properties of bioaerosols generated by respiratory secretions can be expected to affect the efficacy of the decontamination process, and the window of operating conditions affording controlled and consistent properties is not known. Therefore, development and validation of methods that are representative of human respiratory secretions is a necessary condition before one can realistically evaluate techniques for decontamination.

Influenza is commonly thought to be transmitted by three mechanisms (droplet, contact, and aerosol (droplet nuclei)) (CDRF, 2006). Some diseases (e.g., tuberculosis) are known to be mainly transmitted by the droplet nuclei route, whereas droplet transmission is considered by many to be the dominant route for some other diseases (e.g., mumps), although the actual routes are still being debated (Fiegel, Clarke, & Edwards, 2006; Tellier, 2006; Yang et al., 2007). Salgado, Farr, Hall, and Hayden (2002) suggested different roles in influenza between droplet and aerosol transmission. Influenza is mainly spread through droplet transmission by coughing and sneezing from infectious people, while aerosol transmission is important for long-distance and sporadic infection. An infected human can be a source of large droplets generated by coughing and sneezing. During airborne transmission, these droplets will shrink in size with the consequence that both droplets and droplet nuclei contact surfaces. Although many researchers have examined the droplet size generated from humans, the actual size is not clear. Yang et al. (2007) reported that most droplets from coughing, sneezing, and talking have diameter between 1 and 20 μm, and these droplets may contract depending on the humidity and medium generated. Viruses in these droplets can aggregate with each other or be encased by the saliva component, both enhancing persistence of viability. Meanwhile, viability of viruses in saliva can be attenuated by an enzyme action (Diaz-Arnold & Marek, 2002). Therefore, it is important that the transmission medium be factored into the design of the test method.

The focus of this study is to develop a method for reproducibly applying fixed amounts of representative viral particles generated from droplets/aerosols onto FFRs for decontamination testing. This study had specific objectives: (1) to build a droplet/aerosol chamber system that generates droplets/aerosols containing viruses to emulate those from coughing and sneezing, (2) to deliver the droplets and resultant aerosol onto specimens of six commercially available FFRs, and (3) to demonstrate uniformity of deposition within a sample and across independent samples by achieving quarter-to-quarter (Q-T-Q) and sample-to-sample (S-T-S) coefficients of variations (CVs) of less than 20% and 40%, respectively. While the focus of this study was FFRs and a biosafety level (BSL)-I virus, the system was designed to be used with BSL-II microorganisms, which require advanced containment. This fact limited the overall size of the unit, due to the requirement for secondary containment of the test system. The system also has utility outside of FFRs and could be used to load any surface (e.g., a surgical scalpel or glove).

2. Experimental

2.1. Virus and nebulization fluid preparation

MS2 bacteriophage (MS2; ATCC®, 15597-B1™) was applied as the first challenging bioaerosol, because it requires only a BSL-I facility. MS2 has a nonenveloped, icosahedral capsid with a nominal diameter of 27.5 nm (Prescott, Harley, & Klein, 2006; Valegard, Lijas, Fridborg, & Unge, 1990). MS2 infects only male *Escherichia coli* (*E. coli*) and is commonly used as a non-pathogenic surrogate for human pathogenic viruses (e.g., poliovirus, influenza A, and rhinovirus), because of its similarity in resistance to antimicrobial agents and ease of preparation and assay (Aranha-Creado & Brandwein, 1999; Brion & Silverstein, 1999; Fisher, Rengasamy, Viscusi, Vo, & Shaffer, 2009). Freeze-dried MS2 was suspended in deionized (DI) water to a titer of approximately 10^{10}–10^{11} plaque-forming units (PFU) per mL and stored at 4 °C.

Artificial saliva was used as the nebulization fluid to emulate droplets generated by coughing and sneezing. Saliva is a very dilute fluid composed of more than 97% water, plus electrolytes, proteins, and enzymes (Diaz-Arnold & Marek, 2002). A variety of inorganic ions maintain osmotic balance and offer buffering (Diaz-Arnold & Marek, 2002; Dodds, Johnson, & Yeh, 2005; Humphrey & Williamson, 2001). The compounds and their corresponding amounts of artificial saliva are listed in Table 1 (Aps & Martens, 2005; Edward et al., 2004; Veerman, van den Keybus, Vissink, & Nieuw Amerongen, 1996; Wong & Sissions, 2001). Mucin from porcine stomach (Sigma–Aldrich, M1778) was chosen as the representative mucus stimulant (Vingerhoeds, Blijdenstein, Zoet, & Aken, 2005).

Table 1
Composition of artificial saliva (based on 979 mL of DI water).

Chemical species	Amount	Chemical species	Amount
$MgCl_2 \cdot 7H_2O$	0.04 g	KSCN	0.19 g
$CaCl_2 \cdot H_2O$	0.13 g	$(NH_2)_2CO$	0.12 g
$NaHCO_3$	0.42 g	NaCl	0.88 g
0.2 M KH_2PO_4	7.70 mL	KCl	1.04 g
0.2 M K_2HPO_4	12.30 mL	Mucin	3.00 g
NH_4Cl	0.11 g	DMEM[a]	1.00 mL

[a] DMEM: Dulbecco's modified Eagle's medium.

2.2. Test material

Six different models of FFRs approved by NIOSH were employed in this study. Three of those models were also approved by the Food and Drug Administration (FDA) as surgical devices. Each type of FFR has different characteristics, such as number of layers, hydrophilicity, and physical shape. Prior to an FFR testing, 110-mm diameter discs of flat glass-fiber filter (Gelman Science, 61630) were used to determine workable operating conditions of virus concentration, flow rate, and loading time.

2.3. Droplet/aerosol loading system

A droplet/aerosol loading system was custom built for this study with the following requirements: (1) the width and height are less than 120 cm so that it can be placed in a biosafety cabinet; (2) parts can be easily disassembled for sterilization; (3) droplets/aerosols can be distributed uniformly onto substrates; (4) the droplet size distribution is consistent; (5) environmental conditions that can affect the droplet size, such as relative humidity (RH) and temperature, can be controlled. The schematic design of the loading system is shown in Fig. 1. The system consists of a chamber body, an ultrasonic generator (241 T, Sonear®, Farmingdale, NY) for producing the droplets, a bubbler for generating moisture, compressed cylinder air for controlling RH and diluting virus concentrations, an RH meter for measuring humidity, a six-port manifold for distributing the aerosols, a thermometer for measuring temperature, and six supports to hold the flexible-form FFRs during loading (Baron et al., 2008; Feather & Chen, 2003; Fisher et al., 2009). This system can also include a charge neutralizer (Model 3012, TSI Inc., Shoreview, MN). The chamber body was fabricated from stainless steel sheet with welded seams to withstand the high temperature for sterilization. The turntable and six perforated sample plates were employed to increase uniformity of deposition. The particle size distributions (PSDs) were measured by an aerodynamic particle sizer (APS; Model 3321, TSI Inc., Shoreview, MN) through a port on the side of the chamber.

2.4. Chamber operation and determination of operating conditions

Before and after experiments, the chamber was decontaminated by wiping the interior of the chamber with isopropyl alcohol, then allowing the chamber to set for 30 min. Six samples were placed onto the supports on the turntable using sterile forceps. Theoretically, a titer of around 10^7 PFU/mL in the ultrasonic nebulizer with 5-min loading time should provide sufficient loading density ($> 10^3$ PFU/cm^2). The titer was prepared by adding 0.3 mL virus stock suspension into 30 mL artificial saliva. The droplets from the ultrasonic nebulizer after passing the distributor entered the chamber through six inlets. The size of droplets generated and loaded can be affected by the frequency of the ultrasonic generator and by environmental conditions such as RH and temperature. For this study, the frequency of the generator was 2.4 MHz and the environmental conditions were 20 ± 2 °C and 35 ± 5%. Low RH was chosen because the survivability of MS2 is high under this condition. After loading, the residual droplets were allowed to clear for 5 min, and the FFR samples were taken out for extraction and assay.

Various operating parameters were evaluated to determine the conditions that would provide desired droplet characteristics, including loading time (1–30 min), virus titer (10^7–10^8 PFU/mL), turntable speed (0–3 rpm), airflow rate (1–5 Lpm), and mucin concentration (0.3–0.9%). The loading density was controlled by adjusting the loading time and the titer of the virus suspension. To evaluate how viability of the virus is influenced by the ultrasonic process, bioaerosols produced at different times were collected by a Biosampler and their viability was compared. The turntable speed was varied to determine its relationship with uniformity. Flow rate and mucin loading were also varied to investigate their effects on the consistency of delivered droplets. Three runs were carried out for each set of conditions.

After loading with virus, each filter sample was cut into four equal quarters. Each quarter was immersed in 25 mL of extraction medium in a 50-mL conical tube. A 0.25 M glycine solution was applied to extract MS2 from the quarter sample with agitation by a wrist-action shaker (Model 75, Burrell Scientific, Pittsburgh, Pa.) at a 10° angle for 15 min to analyze the loading density (these conditions showed the best extraction efficiency in preliminary testing). The extracted solution was assayed by using the single-layer method (EPA, 1984) to determine the loading density according to Eq. (1) with the

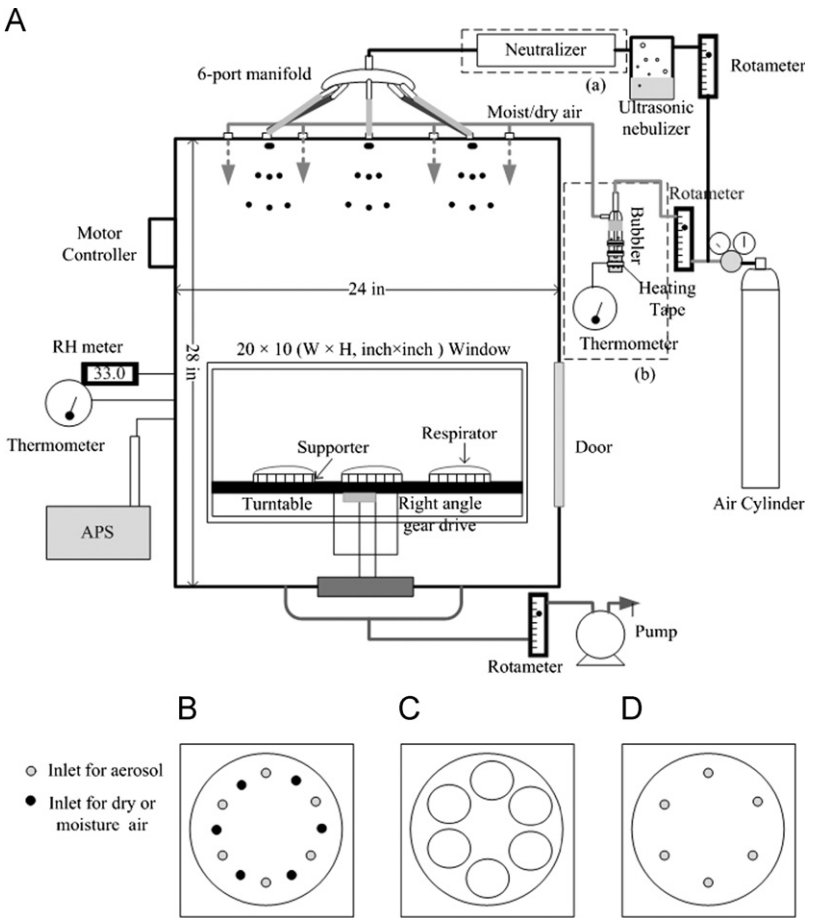

Fig. 1. Schematic diagram of droplet loading system: (A) entire system, (B) distributor on top, (C) turntable, (D) air outlet at bottom ((a) and (b) are needed only in certain conditions).

assumption of 100% extraction efficiency

$$\mathrm{LD} = \frac{\mathrm{PFU}}{10^{-n}} \frac{V_1}{V_2} \frac{4}{\pi d^2} \tag{1}$$

where LD is the loading density, V_1 is the volume of extraction solution, V_2 is the volume of sample, d is the diameter of the filter, and n is the number of dilutions (Lee et al., 2009). To visualize the particle loading, scanning electron microscopy (SEM, JEOL JSM-6330F, JEOL Inc.) of the filter was done before and after loading particles.

2.5. Statistical analysis

The Q-T-Q and S-T-S CVs of loading density were obtained to evaluate the uniformity. R2 8.1 software (CRAN) and Microsoft Excel® were used to calculate one-way analysis of variance (ANOVA) and CV, respectively.

3. Results and discussion

3.1. Determination of operating conditions

The impact of ultrasonic nebulization on viability of virus in the nebulizer reservoir was investigated by measuring the viable counts over time. The results present no significant difference in virus viability between 0 and 30 min (p=0.10) (data not shown). Apparently, the heat shock from ultrasonic vibration did not cause damage to the MS2 in the reservoir during droplet generation. To determine the effect of ultrasonication on virus during droplet generation, viability of the viruses collected in the BioSampler after 5 and 10 min of generation was examined. The theoretical concentration in the BioSampler after 5 min of nebulization is 3×10^5 PFU/mL when the virus titer in the reservoir is 1.0×10^7 PFU/mL. The 5-min time-weighted (0–5 and 5–10 min) average concentration of collected viruses in the BioSampler was approximately

3.2×10^5 PFU/mL, which is similar to the theoretical value. As demonstrated, the ultrasonic nebulizer can be used to produce droplets containing MS2 virus without adverse effects on viability.

Fig. 2a displays the virus loading density as a function of loading time and Fig. 2b shows the loading density as a function of the viral titer. As shown, the loading density had a linear relationship with time and with virus titer in the nebulization medium, as expected based on the initial viability tests. The results show that these two parameters can be adjusted to acquire a desired loading density. It should be noted that in determining the loading density the extracted fraction was assumed to be 1; however, different types of FFRs will have different values that depend on the material property and structure.

The uniformity tests were conducted with the turntable at various speeds because Marple and Rubow (1983) observed increased uniformity of CV from 4.3% to 1.5% when they rotated their aerosol chamber at 0.56 rpm. Fig. 3 shows the CVs from three runs as a function of turntable speed. The variation of the CVs was somewhat larger than Marple and Rubow (1983) reported due to variability working with a viable system (MS2) vs. a non-viable system (PSL and dust).

The flow rate (2 Lpm) of this work is much lower than the rate (100 Lpm) used by Marple and Rubow (1983), and delivers a distribution of droplets that is sufficiently uniform (CV < 20%) even without the turntable, which appears to provide a moderate decrease in CV with increasing rotation rate. The difference among the six positions was not statistically significant (p=0.73) for flat-sheet glass-fiber filters. The reason for this uniformity is likely because settling is the dominant mechanism for large droplets in our system and a six-port distributor delivered the bioaerosols. A straight fog stream was observed through the front window during the loading. Therefore, the turntable speed was not an important parameter to meet the uniformity criteria when the flatsheet filter was employed. The deposition of the particles on FFRs after loading for 1 min was also confirmed by an SEM. As shown in Fig. 4, particles were randomly distributed on fiber surface without any specific pattern.

The criterion for minimum loading density — 10^3 PFU/cm^2 — was achieved for all conditions tested and could be easily increased if needed. Based on these results, the operating conditions to be discussed later were chosen to be 5-min loading time at a titer of 10^7 PFU/mL and 2 rpm turntable speed.

3.2. Droplet size distribution

Fig. 5 shows the size distribution of droplets generated by the ultrasonic nebulizer at different flow rates. The size distributions of droplets generated at 1–3 Lpm were similar, with count median diameters (CMDs) and mass median diameters (MMDs) of 3.5 and 10 μm, respectively. The droplet size distributions at 4 and 5 Lpm were slightly shifted to a smaller diameter. Bimodal distribution was observed in the mass-based size distribution, with modes at 4–6 μm and over 20 μm. The theoretical CMD from the ultrasonic nebulizer can be determined from Eq. (2) (Lang, 1962)

$$d_p(\mathrm{CMD}) = 0.73\sqrt[3]{\frac{\sigma}{\rho f^2}} \tag{2}$$

where d_p is the nebulized droplet size, σ is the surface tension of the liquid, ρ is the density of the liquid, and f is the frequency of the nebulizer. As shown, the droplet size is independent of the flow rate. The gentle airflow within 1–3 Lpm just carries the aerosol away from the liquid surface. However, at a higher flow rate, the larger volume of dry dilution air promotes evaporation, and therefore results in a smaller droplet size. To generate droplets of other sizes, the frequency can

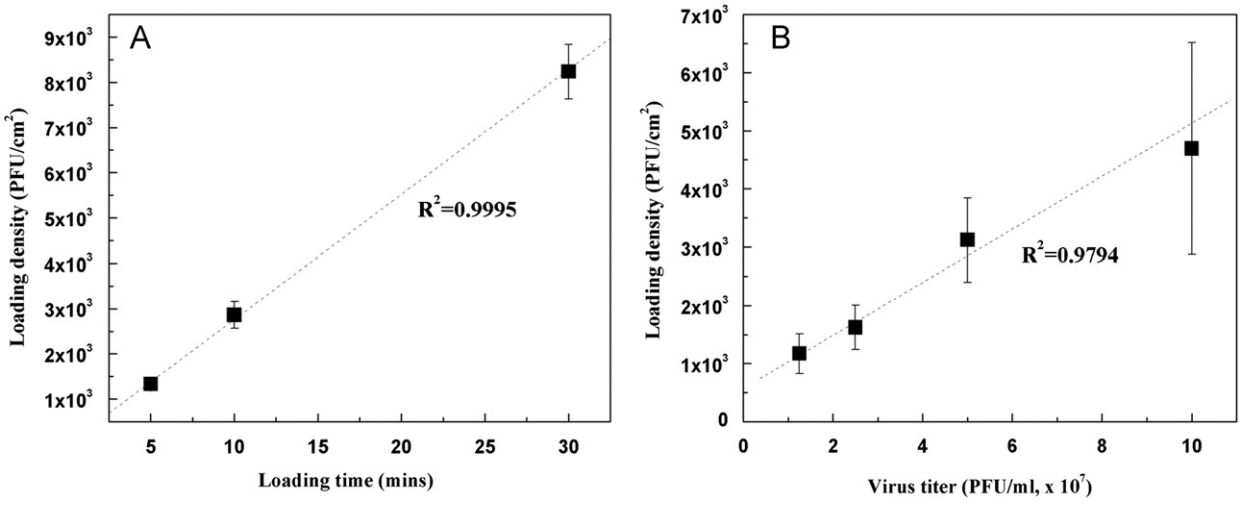

Fig. 2. Loading density as a function of (A) loading time and (B) virus titer in the nebulizer.

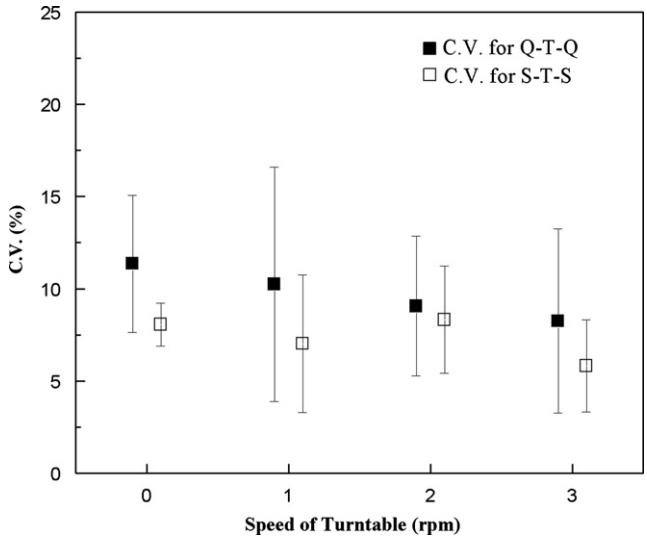

Fig. 3. CVs for Q-T-Q and S-T-S as a function of turntable speed.

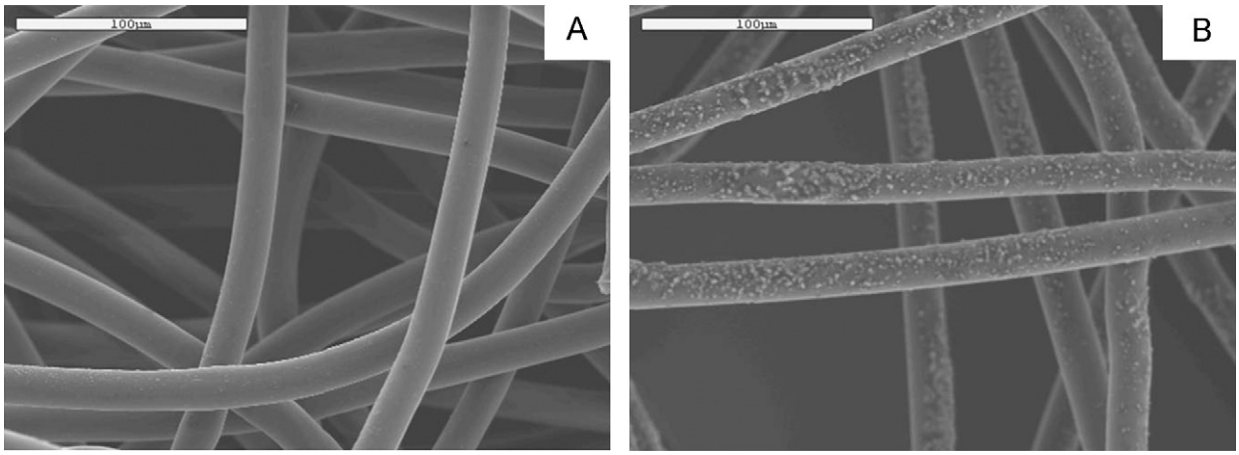

Fig. 4. Scanning electron microscopy images (250 ×) of an FFR (A) before loading and (B) after loading for 1 min.

be adjusted. For example, droplets are expected to be 12.1 and 6.6 times larger, respectively, when lower frequencies of 60 or 150 kHz are used instead of 2.4 MHz (Lang, 1962).

The mucin concentration also plays an important role in determining the initial droplet size because it affects surface tension and density of the artificial saliva used. Mucin at 0.3% was chosen for the artificial saliva in this study to match the protein content in human saliva. Increasing the mucin concentration threefold would reduce the median size to 40% of its original size because of the decrease in surface tension. In summary, the droplet size can be controlled by adjusting the composition of the spray medium, the frequency of the ultrasonic generator, and the flow rate.

The droplet size decreases from the point of generation at the ultrasonic nebulizer all the way to the filter surface due to evaporation, and the size deposited depends on the environmental conditions (i.e., temperature and RH). The flow rates of the ultrasonic generator, dilution air, and temperature of the bubbler can be used to control RH, and heating tape (part (b) in Fig. 1) can be used to adjust the temperature. Fig. 6 displays the droplet size distribution generated and loaded at 2 Lpm through the aerosol generator plus 3 Lpm dry air to provide 35% RH. For this condition, the cylinder air without a bubbler was applied to achieve the low-RH condition. The MMDs for droplets generated and loaded were 9.2 and 3.2 μm, respectively, with corresponding CMDs of 3.4 and 1.8 μm, which are similar to the droplet size reported in the literature (Yang et al., 2007; Morawska et al. 2009) to have been generated by humans. The droplet's residence time is 0.13 s when settling is considered the main mechanism acting in this chamber. The droplet's theoretical lifetime at 35% RH is around 0.15 s, which means that droplets just reaching the FFR are almost completely evaporated. The size of a completely evaporated droplet can be calculated according to Eq. (3)

$$d_p = d_d \sqrt[3]{F_v} \tag{3}$$

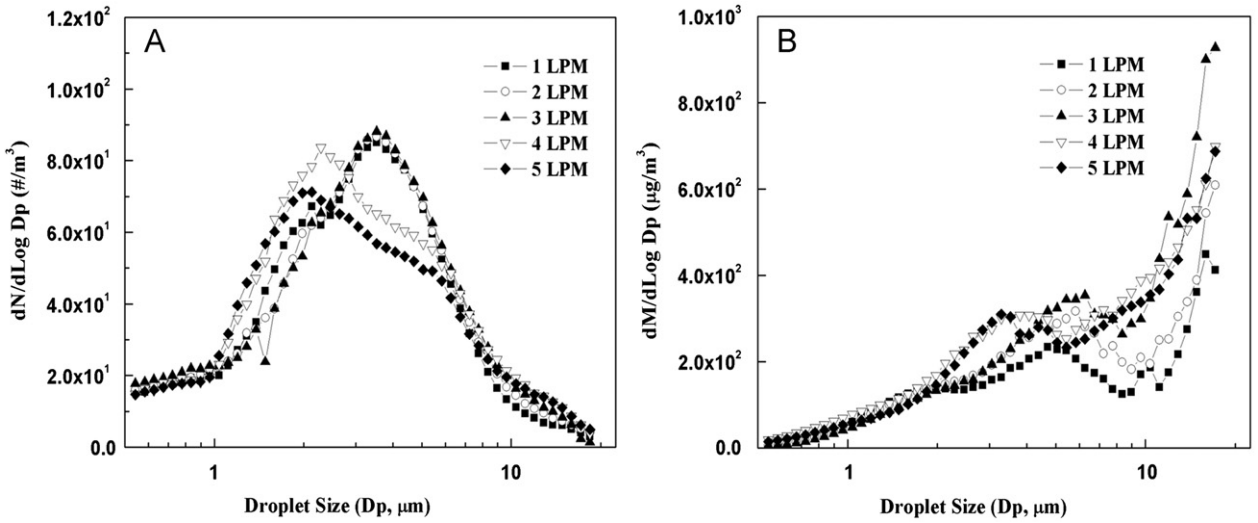

Fig. 5. (A) Number- and (B) mass-based size distribution of droplets generated by ultrasonic nebulizer at five flow rates.

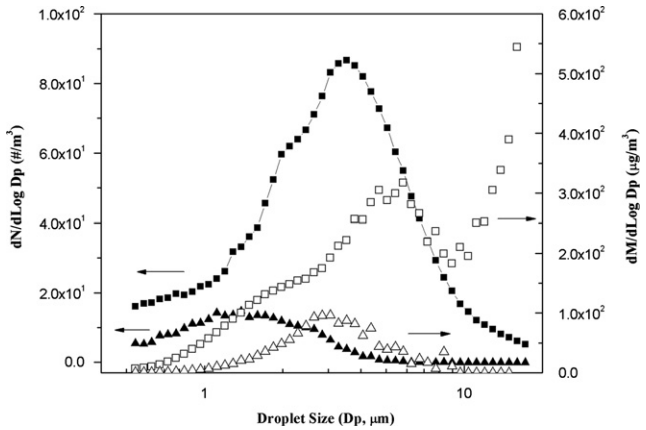

Fig. 6. The number- and mass-based particle size distribution of generated droplets and loaded droplets at 2 Lpm through the aerosol generator plus 3 Lpm dry air and 2-rpm turntable speed.

Table 2
Loading density and CVs of Q-T-Q and S-T-S for six different FFRs (N=3, criteria of CV for Q-T-Q and S-T-S: 20% and 40%, respectively).

Shape	Type	No.	Loading density (PFU/cm^2)	CV for Q-T-Q (%)	CV for S-T-S (%)
Fixed	P[††]	1	$2.3\times10^3\pm0.3\times10^3$	12.07 ± 2.74	9.05 ± 2.22
	P	2	$2.9\times10^3\pm0.2\times10^3$	10.92 ± 2.09	5.89 ± 0.68
	S[‡‡]	3	$1.0\times10^3\pm0.1\times10^3$	15.41 ± 6.89*	10.12 ± 3.75*
	P	4	$2.6\times10^3\pm0.2\times10^3$	18.04 ± 2.97	6.94 ± 3.26
Flexible (duckbill)	S	5	$1.2\times10^3\pm0.1\times10^3$	13.70 ± 1.59	9.17 ± 3.86
	S	6	$1.8\times10^3\pm0.2\times10^3$	13.19 ± 7.19	10.27 ± 1.71

[††] P: particulate respirator.
[‡‡] S: surgical respirator.
* N=2.

where d_p is the diameter of the aerosol particle and F_v is the volume fraction of solid material in the suspension in the nebulizer. For 0.3% mucin, the volume fraction is 2.08×10^{-2}, so d_p is calculated to be 2.6 μm when d_d is 9.2 μm. The reason the measured value is higher than the theoretical value is an incomplete evaporation. After running the experiment, we noted that the filter surface was slightly damp, which is consistent with the above interpretation.

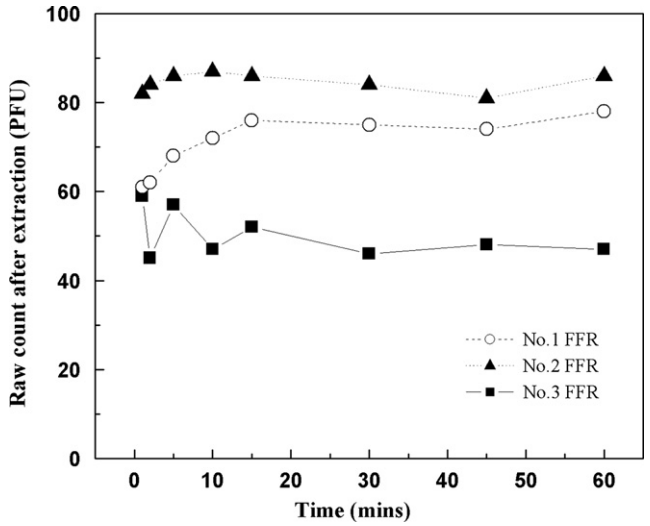

Fig. 7. Recovery of viable MS2 as a function of extraction time for three FFRs.

3.3. Loading onto NIOSH-certified FFRs

The CVs for uniform deposition of droplets/aerosols onto substrates for six different FFRs were calculated by analyzing the infectivity of viruses extracted from the loaded filter (Table 2). The flexible nature of the FFRs makes it difficult to achieve deposition on the same spot with the same shape each time. Therefore, a holding medium is necessary to achieve low CV values. Even for fixed-form FFRs, some inherently cannot produce equal quarters because the shape is not symmetric. Operational variation while cutting the sample (e.g., uneven quarters) can also contribute to larger CV values. Consequently, the CV for Q-T-Q was higher than that for S-T-S over all FFRs. It is possible to use circular areas punched from an FFR so that the difference in shape will not influence the results. However, this was outside the scope of the study, which aimed to evaluate decontamination effectiveness using an entire FFR. Nevertheless, the average CVs for both Q-T-Q and S-T-S for all FFRs were lower than the criteria — 20% and 40%, respectively — demonstrating the system's ability to consistently load the test agents. Table 2 also displays the results of the loading densities. As shown, all sets had sufficient quantity to meet the threshold criteria.

Due to differences in surface properties, the loading density of different respirator models can be different even when the same operating conditions are applied. Fig. 7 shows the extraction efficiency of three different FFRs at various extraction times. Different layer structures and properties of the FFRs are responsible for the differences as discussed. The shape of the FFR is another reason for differences in loading density. The loading density reported in Table 2 was calculated based on the FFR's projected area. The FFR, having a duck-bill shape, showed a lower loading density owing to its different curvature. As shown, both factors can affect loading density. Nevertheless, the loading density can be easily met in a controlled fashion using the specified conditions, and can be conveniently increased by adjusting the loading time, virus titer, or both.

4. Conclusions

A simple system for producing, delivering, and loading of consistent challenges of droplets/aerosols containing virus onto FFRs has been developed and assessed. The respective CVs for S-T-S and Q-T-Q for the six NIOSH-certified FFRs tested were 8.57 and 13.89, lower than the criteria — 20% and 40%, respectively. The droplet size can be altered by tuning the frequency of the ultrasonic nebulizer, by changing the composition of the dispersion aerosolized, and by adjusting the temperature and RH inside the chamber. Droplets emulating bioaerosols released during coughing and sneezing can be produced using specific conditions and the loading density can be achieved by controlling the loading time and the virus titer in the nebulization medium. This system allows for development and validation of a standard method for loading bioaerosol challenges when different decontamination techniques are to be compared. It also has utility for loading surfaces to study fomite transmission and reaerosolization of particles from surfaces. It can be further applied to generate and load droplets and aerosols of different sizes and to load onto materials other than FFRs.

Acknowledgements

This research was supported by the Air Force Research Laboratory through Contract no. FA8650-06-C5913. The authors are grateful to Profs. Dale Lundgren (University of Florida) and Virgil Marple (University of Minnesota) for providing

valuable comments on the design of the delivery chamber and to the Major Analytical Instrumentation Center, Department of Materials Science and Engineering at the University of Florida for providing the SEM. The authors also wish to acknowledge Ken Reed (TMR, Gainesville) for building the chamber for this project. Myung-Heui Woo acknowledges the Alumni Scholarship from the University of Florida for partial financial support.

References

Aps, J. K.M., & Martens, L. C. (2005). Review: The physiology of saliva and transfer of drugs into saliva. *Forensic Science International*, *150*, 119–131.

Aranha-Creado, H., & Brandwein, H. (1999). Application of bacteriophages as surrogates for mammalian viruses: a case for use in filter validation based on precedents and current practices in medical and environmental virology. *Journal of Pharmaceutical Science and Technology*, *53*, 75–82.

Baron, P., Estill, C., Deye, G., Hein, M., Beard, J. Larsen, L., et al. (2008). Development of an aerosol system for uniformly depositing *Bacillus anthracis* spore particles on surfaces. *Aerosol Science and Technology*, *42*, 159–172.

Brion, G. M., & Silverstein, J. (1999). Iodine disinfection of a model bacteriophage, MS2, demonstrating apparent rebound. *Water Research*, *33*, *169*–179.

CDC (2009). Fact sheet: novel H1N1 flu situation update. Available at 〈http://www.cdc.gov/h1n1flu.update.htm〉, September 15, 2008.

CDRF, J. (2006). *Reusablility of Facemasks during an Influenza Pandemic: Facing the Flu*. Washington DC: National Academies Press.

Diaz-Arnold, A. M., & Marek, C. A. (2002). The impact of saliva on patient care: a literature review. *The Journal of Prosthetic Dentistry*, *88*, 337–343.

Dodds, M. W.J., Johnson, D. A., & Yeh, C. K. (2005). Health benefit of saliva: a review. *Journal of Dentistry*, *33*, 223–233.

Edward, D., Man, J., Brand, P., Kaststra, J., Sommerer, K. Stone, H., et al. (2004). Inhaling to mitigate exhaled bioaerosols. *Proceedings of the National Academy of Sciences*, *101*, 17383–17388.

EPA (1984). USEPA manual methods for virology. *US Environmental Protection Agency, Research and Development*, 600/4-84-013, Cincinnati, OH.

Feather, G., & Chen, B. (2003). Design and use of a settling chamber for sampler evaluation under calm-air conditions. *Aerosol Science and Technology*, *37*, 261–270.

Fiegel, J., Clarke, R., & Edwards, D. A. (2006). Airborne infectious disease and the suppression of pulmonary bioaerosols. *Drug Discovery Today*, *11*, 51–57.

Fisher, E., Rengasamy, S., Viscusi, D., Vo, E., & Shaffer, R. (2009). Development of a test system to apply virus containing particles to filtering facepiece respirators for the evaluation of decontamination procedure. *Applied and Environmental Microbiology*, *75*, 1500–1507.

Humphrey, S. P., & Williamson, R. T. (2001). A review of saliva: normal composition, flow and function. *Journal of Prosthetic Dentistry*, *85*, 162–169.

Lang, R. (1962). Ultrasonic atomization of liquid. *Journal of the Acoustical Society of America*, *34*, 6–8.

Lee, J. H., Wu, C. Y., Lee, C., Anwar, D., Wysocki, K. Lungren, D., et al. (2009). Assessment of iodine-treated filter media for removal and inactivation of MS2 bacteriophage aerosols. *Journal of Applied Microbiology*, *107*, 1912–1923.

Marple, V., & Rubow, K. (1983). An aerosol chamber for instrument evaluation and calibration. *The American Industrial Hygiene Association Journal*, *44*, 361–367.

Morawska, L., Johnson, G., Ristovski, Z., Hargreaves, M., Mengersen, K. Corbett, S., et al. (2009). Size distribution and sites of origin of droplets expelled from the human respiratory tract during expiratory activities. *Journal of Aerosol Science*, *49*, 256–269.

Prescott, L. M., Harley, J. P., & Klein, D. A. (2006). *Microbiology*. New York, NY: McGraw–Hill Companies, Inc.

Salgado, C. D., Farr, B. M., Hall, K. K., & Hayden, F. G. (2002). Influenza in the acute hospital setting. *The Lancet Infectious Diseases*, *2*, 145–155.

Tellier, R. (2006). Review of aerosol transmission of influenza. *Emerging Infectious Diseases*, *12*, 1657–1661.

Valegard, K., Lijas, L., Fridborg, K., & Unge, T. (1990). The three-dimensional structure of the bacterial virus MS2. *Nature*, *345*, 36–41.

Veerman, E. C.I., van den Keybus, P. A.M., Vissink, A., & Nieuw Amerongen, A. V. (1996). Human glandular salivas: their separate collection and analysis. *European Journal of Oral Science*, *104*, 346–352.

Vingerhoeds, M. H., Blijdenstein, T. B.J., Zoet, F. D., & Aken, G. A.V. (2005). Emulsion flocculation induced by saliva and mucin. *Food Hydrocolloids*, *19*, 915–922.

WHO (2010). Pandemic (H1N1) 2009 - update 108. Available at 〈http://www.who.int/csr/don/2010_07_09/en/index.html〉, accessed on July 09, 2010.

Wong, L., & Sissions, C. H. (2001). A comparison of human dental plaque microcosm biofilms grown in an undefined medium and a chemically defined artificial saliva. *Archives of Oral Biology*, *46*, 477–486.

Yang, S. H., Lee, G. W.M., Chen, C. M., Wu, C. C., & Yu, K. P. (2007). The size and concentration of droplets generated by coughing in human subjects. *Journal of Aerosol Medicine*, *20*, 484–494.